

**Observing the  
continental-scale  
carbon balance**

T. Kaminski et al.

This discussion paper is/has been under review for the journal Atmospheric Chemistry and Physics (ACP). Please refer to the corresponding final paper in ACP if available.

# Observing the continental-scale carbon balance: assessment of sampling complementarity and redundancy in a terrestrial assimilation system by means of quantitative network design

T. Kaminski<sup>1</sup>, P. J. Rayner<sup>2</sup>, M. Voßbeck<sup>1</sup>, M. Scholze<sup>3</sup>, and E. Koffi<sup>4</sup>

<sup>1</sup>FastOpt, Lerchenstraße 28a, 22767 Hamburg, Germany

<sup>2</sup>School of Earth Sciences, University of Melbourne, Melbourne, Australia

<sup>3</sup>Dep. of Earth Sciences, University of Bristol, Bristol, UK

<sup>4</sup>LSCE/IPSL, Gif-sur-Yvette Cedex, France

Received: 29 February 2012 – Accepted: 1 March 2012 – Published: 12 March 2012

Correspondence to: T. Kaminski (thomas.kaminski@fastopt.com)

Published by Copernicus Publications on behalf of the European Geosciences Union.

Title Page

Abstract

Introduction

Conclusions

References

Tables

Figures

◀

▶

◀

▶

Back

Close

Full Screen / Esc

Printer-friendly Version

Interactive Discussion



## Abstract

This paper investigates the relationship between the heterogeneity of the terrestrial carbon cycle and the optimal design of observing networks to constrain it. We combine the methods of quantitative network design and carbon-cycle data assimilation to a hierarchy of increasingly heterogeneous descriptions of the European terrestrial biosphere as indicated by increasing diversity of plant functional types. We employ three types of observations, flask measurements of CO<sub>2</sub> concentrations, continuous measurements of CO<sub>2</sub> and pointwise measurements of CO<sub>2</sub> flux. We show that flux measurements are extremely efficient for relatively homogeneous situations but not robust against increasing or unknown complexity. Here a hybrid approach is necessary and we recommend its use in the development of integrated carbon observing systems.

## 1 Introduction

CO<sub>2</sub> and methane are the most important anthropogenic greenhouse gases. Their increasing concentration is the major reason for global warming (Solomon et al., 2007). It is thus of paramount interest to quantify and ultimately predict the exchanges of these gases between the terrestrial biosphere and the atmosphere. At a number of points on the globe, carbon and water fluxes are sampled directly (see, e.g., <http://www.fluxnet.ornl.gov>). The interpolation of these measurements to the globe (up-scaling) requires external information about the uncertain spatio-temporal flux structure. The same type of information is required by atmospheric transport inversions (see, e.g., Rayner et al., 1999; Gurney et al., 2002; Enting, 2002) which infer surface fluxes from atmospheric concentration measurements. The most sophisticated tools for quantifying the structure and variability of carbon fluxes are process models of the terrestrial carbon cycle like those used for the assessments of the IPCC (Solomon et al., 2007). Underlying these models is the assumption of fundamental equations that govern the processes controlling the terrestrial carbon fluxes. Uncertainty in the simulation

ACPD

12, 7211–7242, 2012

## Observing the continental-scale carbon balance

T. Kaminski et al.

Title Page

Abstract

Introduction

Conclusions

References

Tables

Figures



Back

Close

Full Screen / Esc

Printer-friendly Version

Interactive Discussion



**Observing the  
continental-scale  
carbon balance**

T. Kaminski et al.

Title Page

Abstract

Introduction

Conclusions

References

Tables

Figures

◀

▶

◀

▶

Back

Close

Full Screen / Esc

Printer-friendly Version

Interactive Discussion



of these fluxes arises from four sources: first, there is uncertainty in the forcing data (such as precipitation or temperature) driving the terrestrial processes. Second, there is uncertainty regarding the formulation of individual processes and their numerical implementation (structural uncertainty). Third, there are uncertain constants (process parameters) in the formulation of these processes. Forth, there is uncertainty about the state of the terrestrial biosphere at the beginning of the simulation.

Observational information helps to reduce these uncertainties. Currently there are several initiatives to extend the observational network of the carbon cycle. Europe's Integrated Carbon Observing System (ICOS, see <http://www.icos-infrastructure.eu/>), for example, aims at setting up an integrated sampling network for land, ocean, and atmosphere. Ideally, all data streams are interpreted simultaneously with the process information provided by the model to yield a consistent picture of the carbon cycle that balances all the observational constraints, thereby taking the respective uncertainty ranges into account. Data assimilation systems around prognostic models of the carbon cycle are the ideal tools for this integration allowing us to assimilate a wide range of observations. They can, for example, be applied to systematically reduce parametric uncertainty (Kaminski et al., 2002, e.g.) or to expose structural errors (Rayner, 2010). In a first step, they use the observations to constrain the uncertain process parameters (calibration), and in a second step they use the calibrated model for analysis and prediction. Ideally, both steps include the propagation of uncertainties. This allows us to derive uncertainty ranges on simulated *target quantities* that are consistent with the uncertainties in the observations and the model. Examples of such target quantities are fluxes of carbon on regional, continental, or global scale, integrated over part of the assimilation period (*diagnostic target quantity*) or some period before or after (*prognostic target quantity*). With regard to a specified target quantity, such an assimilation system can assess the performance of a given observational network. This performance is typically quantified by the uncertainty range.

Quantitative Network Design (QND) aims at constructing an observational network with optimal performance. The approach is based on Hardt and Scherbaum (1994)

**Observing the  
continental-scale  
carbon balance**

T. Kaminski et al.

Title Page

Abstract

Introduction

Conclusions

References

Tables

Figures

◀

▶

◀

▶

Back

Close

Full Screen / Esc

Printer-friendly Version

Interactive Discussion



who optimised the station locations for a seismographic network. It was first applied to observational networks of the global carbon cycle by Rayner et al. (1996), who optimised the locations of atmospheric CO<sub>2</sub> and δ<sup>13</sup>C measurements. A pioneering study for sensor design has been performed by Rayner and O'Brien (2001) who established the required precision for observations of the column-integrated atmospheric CO<sub>2</sub> concentration from space.

The latter two studies investigated purely atmospheric networks. To assist the design of an integrated carbon observing system, we need the capability of evaluating the complementarity of various observational data streams including those of the terrestrial biosphere. As outlined by Kaminski and Rayner (2008) assimilation systems are the ideal tool for this task. The Carbon Cycle Data Assimilation System (CCDAS, see <http://ccdass.org>) can assimilate several observational data streams and infers uncertainty ranges on diagnosed (Rayner et al., 2005) or prognosed carbon (Scholze et al., 2007; Rayner et al., 2011) and water (Kaminski et al., 2011) fluxes. The first QND applications investigated the utility of space borne observations of atmospheric CO<sub>2</sub> (Kaminski et al., 2010) or vegetation activity (Kaminski et al., 2011) in constraining various surface fluxes. Another study explores the atmospheric in situ network and its ability to constrain the productivity of the terrestrial biosphere (Koffi et al., 2012).

Kaminski and Rayner (2008) noted two general aspects of QND studies. The first (Rayner et al., 1996) is the dependence on the target quantity; clearly different networks are optimal for constraining different things. The second is the dependence on prior knowledge brought to the problem. For traditional inversions of fluxes this information takes the form of the prior covariance. For CCDAS it is determined by the process resolution of the underlying dynamical model (how many processes are modelled) and the spatial detail at which these processes are allowed to vary independently. The level of heterogeneity of the biosphere is a fundamental question which goes beyond CCDAS; it determines how much any understanding of processes gained locally can be more widely applied. However it is clear that observing networks presupposing a given heterogeneity are at some risk. This paper uses the network designer, a CCDAS-based

interactive QND tool, to investigate the performance of several networks composed of direct flux observations and flask or continuous samples of the atmospheric carbon dioxide concentration. In particular we investigate the robustness of these networks to various choices of target quantities and levels of heterogeneity.

5 The outline of the paper is as follows. Section 2 describes our QND methodology and Sect. 3 the networks we consider. Then Sect. 4 will present and discuss the evaluations. Finally, in Sect. 5 we summarise our conclusions.

## 2 Methods

10 CCDAS is built around the Biosphere Energy Transfer HYdrology scheme (BETHY, Knorr, 2000; Knorr and Heimann, 2001), a global model of the terrestrial vegetation. The version used here is described in Rayner et al. (2005). This section gives brief descriptions of BETHY, the observational data types, CCDAS and of the QND approach.

### 2.1 BETHY

15 Following Wilson and Henderson-Sellers (1985) BETHY decomposes the global terrestrial vegetation into 13 Plant Functional Types (PFTs) as listed in Table 1. Each grid cell can be covered by up to three PFTs. Figure 1 shows the distribution of the dominant PFT. As in Scholze et al. (2007) we integrate the model over 21 yr from 1979 to 1999 on a global 2 by 2 degree grid and use observed meteorological driving data (Nijssen et al., 2001).

20 The process formulations within BETHY are controlled by a set of process parameters (see Table 2). For this study we use the model version of Scholze et al. (2007) with the extension of simulating hourly Net Ecosystem Productivity (NEP). This is done by dividing the daily calculated heterotrophic respiration flux into 24 equal-sized hourly fluxes and subtracting these fluxes from the hourly simulated Net Primary Productivity (NPP). BETHY simulates 13 PFTs including 21 different parameters. Three of these

## Observing the continental-scale carbon balance

T. Kaminski et al.

Title Page

Abstract

Introduction

Conclusions

References

Tables

Figures



Back

Close

Full Screen / Esc

Printer-friendly Version

Interactive Discussion



parameters are PFT-specific and 18 are applied globally, i.e. they refer to all PFTs. We thus have  $18 + 3 \times 13 = 57$  parameters. The role of the individual parameters is described elsewhere (Rayner et al., 2005; Scholze et al., 2007). In our context of network design it is important to know to which parameters our respective target quantities are sensitive. We will use regional integrals of the NPP and the NEP as target quantities. The latter is net CO<sub>2</sub> flux between the atmosphere and the biosphere and defined as the difference of NPP and heterotrophic soil respiration. Except for one atmospheric parameter  $c_0$ , all parameters impact NEP. NPP is sensitive to all parameters, except  $c_0$  and the soil and carbon balance parameters.

## 2.2 Observational data types

In this study we use three types of observational data: direct (NEP) flux measurements, flask and continuous samples of the atmospheric CO<sub>2</sub> concentration. Within the model, a flux measurement is represented by a time series of hourly NEP samples of the grid cell the site is located in. The atmospheric data types require, as a so-called observation operator, an atmospheric transport model to transform the global NEP field into atmospheric concentrations. Flask samples are represented by a time series of monthly mean concentrations at the sampling location as simulated by the atmospheric transport model TM2 (Heimann, 1995), which is run at 8 by 10 degree horizontal resolution and with nine vertical levels. As in Carouge et al. (2010a,b) continuous samples are represented by a time series of daily mean concentrations at the sampling location as simulated by the atmospheric transport model LMDZ (Hauglustaine et al., 2004), which is run at 3.75 by 2.5 degree resolution over most of the globe but a zoomed 0.5 degree resolution over Europe. For each data type the observational time series covers the 20 yr period from 1980 to 1999.

## Observing the continental-scale carbon balance

T. Kaminski et al.

Title Page

Abstract

Introduction

Conclusions

References

Tables

Figures



Back

Close

Full Screen / Esc

Printer-friendly Version

Interactive Discussion



## 2.3 CCDAS

CCDAS uses a gradient method to adjust BETHY's process parameters in order to minimise a cost function. This cost function quantifies the fit to all observations plus the deviation from prior knowledge on the process parameters:

$$J(\tilde{\mathbf{x}}) = \frac{1}{2} \left[ (M(\tilde{\mathbf{x}}) - \mathbf{d})^T \mathbf{C}(d)^{-1} (M(\tilde{\mathbf{x}}) - \mathbf{d}) + (\tilde{\mathbf{x}} - \mathbf{x}_0)^T \mathbf{C}(x_0)^{-1} (\tilde{\mathbf{x}} - \mathbf{x}_0) \right] \quad (1)$$

where  $M$  denotes the model considered as a mapping from parameters to observations,  $d$  the observations with data uncertainty  $\mathbf{C}(d)$ ,  $x_0$  the prior parameter values with uncertainty  $\mathbf{C}(x_0)$ , and the superscript  $T$  the transpose.

The second derivative (Hessian) of the cost function at the optimum  $x$  is used to approximate the inverse of the covariance matrix  $\mathbf{C}(x)$  that quantifies the uncertainty ranges on the parameters that are consistent with uncertainties in the observations and the model. In a second step, the linearisation  $\mathbf{N}'$  (Jacobian) of the model  $N$  used as a mapping from parameters to target quantities is used to propagate the parameter uncertainties forward to the uncertainty in a target quantity  $\sigma(y)$ :

$$\sigma(y)^2 = \mathbf{N}' \mathbf{C}(x) \mathbf{N}'^T + \sigma(y_{\text{mod}})^2. \quad (2)$$

$\sigma(y_{\text{mod}})$  quantifies all uncertainty in the simulation of the target quantity except the uncertainty in  $x$  (which we resolve explicitly). If the model was perfect,  $\sigma(y_{\text{mod}})$  would be zero. In contrast, if the parameters were perfectly known, the first term on the right hand side would be zero. Likewise the data uncertainty  $\mathbf{C}(d)$  is the sum of the observational uncertainty and all uncertainty in the simulation of the observations except the uncertainty in the parameter vector.

All derivative information is provided with the same numerical accuracy as the original model in an efficient form via automatic differentiation of the model code by the automatic differentiation tool TAF (Giering and Kaminski, 1998).

### Observing the continental-scale carbon balance

T. Kaminski et al.

Title Page

Abstract

Introduction

Conclusions

References

Tables

Figures



Back

Close

Full Screen / Esc

Printer-friendly Version

Interactive Discussion



## 2.4 QND

In network design mode, CCDAS is restricted to the uncertainty propagation for candidate networks. It builds on the optimal parameter set estimated from data of the available network for the evaluation of the required first and second derivatives. In our case the optimal parameter vector is taken from the study of Scholze et al. (2007). For the evaluation of potential networks, the Hessian is evaluated for  $d = M(x)$ . In this case the posterior target uncertainty solely depends on the prior and data uncertainties and linearised model responses at observational locations and for target quantities. The approach does not require real observations, and can thus evaluate hypothetical candidate networks (see Kaminski and Rayner, 2008; Kaminski et al., 2010). Candidate networks are defined by a set of observations characterised by observational data type, location, and data uncertainty. In practise for pre-defined target quantities and observational types and locations, model sensitivities can be pre-computed and stored. A network composed of these pre-defined observations, can then be evaluated in terms of the pre-defined target quantities without further model evaluations. Only matrix algebra is required to combine the pre-computed sensitivities with the data uncertainties.

This is the approach implemented in the network designer (see <http://imecc.ccdas.org>), an interactive software tool that evaluates networks composed of flask and continuous samples of atmospheric CO<sub>2</sub> and direct flux measurements. Available target quantities are NPP and NEP over three regions: Europe, Brazil, and Russia. They are provided in the form of annual mean values averaged over the 20 yr assimilation period. Model sensitivities have been pre-computed for a list of atmospheric sampling sites (see Fig. 2 and Table 4). For flux measurements, model sensitivities have been pre-computed for every terrestrial grid cell and all PFTs that are available in the grid cell. When defining the site, the user can specify a mix among these PFTs. Uncertainties for data sampled at different sites and times are assumed to be uncorrelated. The uncertainty for each site is quantified by a standard deviation  $\sigma(d)$ , that reflects the

## Observing the continental-scale carbon balance

T. Kaminski et al.

Title Page

Abstract

Introduction

Conclusions

References

Tables

Figures

⏪

⏩

◀

▶

Back

Close

Full Screen / Esc

Printer-friendly Version

Interactive Discussion



combined effect of observational  $\sigma(d_{\text{obs}})$  and model error  $\sigma(d_{\text{mod}})$ :

$$\sigma(d)^2 = \sigma(d_{\text{obs}})^2 + \sigma(d_{\text{mod}})^2 \quad (3)$$

The unit of the data uncertainties depends on the data type. For flask and continuous samples of atmospheric CO<sub>2</sub> it is ppm, for eddy flux measurements it is gC m<sup>-2</sup> day<sup>-1</sup> (where gC stands for grams of carbon). The output of the network designer is the list of posterior uncertainties  $\sigma(y)$  of the target quantities according to Eq. (2).  $\sigma(y_{\text{mod}})$  can be specified by the user as a percentage of the 20 yr average of annual mean NPP.

### 3 Experimental setup

We will be evaluating several networks. To define these networks we have to select the sampling locations and the respective data uncertainties. To simplify the discussion, we choose a uniform data uncertainty for each data type. The contribution from model error should not be specific to the models we are using but more general. After all the observational networks should not be designed for interpretation by a specific model but rather for a typical state-of-the-art model.

For the flux measurements we use an uncertainty of 10 gC m<sup>-2</sup> day<sup>-1</sup>. Compared to the minimum uncertainty of  $3 \times 10^{-6} \text{ mol m}^{-2} \text{ s}^{-1} \approx 3.11 \text{ gC m}^{-2} \text{ day}^{-1}$  of Knorr and Kattge (2005) this may appear conservative. It seems, however, fair to assume this value for the 20 yr time series, because our uncertainty has to account for the effect that nighttime samples are typically not used, and for correlations in observational uncertainty and in model uncertainty.

For the atmospheric flask samples we use an uncertainty of 1.0 ppm. This value is also higher than the pure observational uncertainty but, again, it must also account for the combined error in the terrestrial and transport models. With the same reasoning we use an uncertainty of 1.5 ppm for the continuous observations, which are more difficult to simulate.

## Observing the continental-scale carbon balance

T. Kaminski et al.

Title Page

Abstract

Introduction

Conclusions

References

Tables

Figures

⏪

⏩

◀

▶

Back

Close

Full Screen / Esc

Printer-friendly Version

Interactive Discussion



Next we have to define the sampling locations. For each observational data type we define a base network:

- The atmospheric flask sampling network *flask*, which consists of the 41 monitoring stations listed in Table 2 of Kaminski et al. (2002) and shown in Fig. 2.
- The atmospheric continuous sampling network *cont*, which consists of the 15 sites listed in Table 4 and indicated with symbol “X” in Fig. 3.
- The eddy flux network *flux*, which consists of a dedicated site for each of the ten PFTs that are available to the model over Europe (PFT numbers 3–5 and 7–13 of Table 1). Each site is defined such that it is covered to 100 % by the respective PFT. Table 3 lists the sites and Fig. 3 indicates their locations with the symbols “+”.

We evaluate the networks in terms of the uncertainty reduction (Kaminski et al., 1999) in six target quantities:

$$1 - \frac{\sigma(y)}{\sigma(y_{\text{prior}})}, \quad (4)$$

where  $\sigma(y_{\text{prior}})$  denotes the uncertainty in the target quantity without any observational constraint and  $\sigma(y)$  is taken from Eq. (2). The prior uncertainties for our target quantities are 0.45 GtC, 1.45 GtC, and 1.13 GtC for NEP over Europe, Russia, and Brazil, respectively, and 0.66 GtC, 1.08 GtC, and 4.86 GtC for NPP.  $\sigma(y_{\text{mod}})$  is an offset in Eq. (2). If the term was very high it would dominate the posterior uncertainty. To render the contrasts between the networks more drastic, we use a value of zero, i.e. we only analyse the effect of the networks on the parametric uncertainty in the target quantities.

## Observing the continental-scale carbon balance

T. Kaminski et al.

[Title Page](#)[Abstract](#)[Introduction](#)[Conclusions](#)[References](#)[Tables](#)[Figures](#)[◀](#)[▶](#)[◀](#)[▶](#)[Back](#)[Close](#)[Full Screen / Esc](#)[Printer-friendly Version](#)[Interactive Discussion](#)

## 4 Results and discussion

We start this section with evaluations of simple networks composed of one or two flux sites. Then we move on to the base networks defined in Sect. 3 and, finally, study the effect of increasing the number of PFTs that are available to the model.

### 4.1 Simple configurations of flux sites

The selection of a site location for sampling a particular PFT defines the Jacobian matrix that provides the link from the model parameters (required for simulating that PFT) to the simulated flux. To understand the effects which we will later see in larger networks, it is instructive to evaluate first a series of small networks consisting of one or two flux sites. We start with the separate evaluation of two sites which both observe PFT 9 (C3 grass) to 100 %, namely “site1731-9” in Southern Spain and “site143-9” in Northern Scandinavia (see Table 3 for site locations), for convenience in the following just referred to as sites “143” and “1731”. The respective uncertainty reductions are displayed by blue (site “143”) and orange (site “1731”) bars in Fig. 4. First we note that flux measurements over Europe can reduce the uncertainty of target quantities over Russia and Brazil. This reflects our assumption of fundamental processes with a combination of universal and PFT-specific parameters. An observation at any site provides information that reduces uncertainty anywhere. Figure 5 shows for site “1731” the uncertainty reduction in NEP per grid cell. This quantifies how the observational information of the site is spread around the globe. Comparing with Fig. 1 we note high uncertainty reduction where the dominant PFT is C3 grass.

Among the two sites in terms of NEP site “1731” performs only marginally better, but in terms of NPP it performs about 10 percentage points better.<sup>1</sup> Next we investigate the complementarity between the two sites, i.e. we use a network that consists of both

<sup>1</sup>The unit *percentage point* quantifies an absolute change in the percentage value. For example, for a value of 40 % an increase by 50 percentage points yields 90 %. By contrast, an increase by 50 % corresponds to 20 percentage points and yields 60 %.

## Observing the continental-scale carbon balance

T. Kaminski et al.

Title Page

Abstract

Introduction

Conclusions

References

Tables

Figures

◀

▶

◀

▶

Back

Close

Full Screen / Esc

Printer-friendly Version

Interactive Discussion



sites and note a slight improvement for NPP over Europe and Russia (yellow bar in Fig. 4) compared to the better site “1731” alone. For these two target quantities the weaker site “143” is not *redundant* in this two site network, because it brings at least a little bit of extra information. In other words there is at least a slight *complementarity* between the two sites with respect to the two target quantities.

For the analysis of the above effects, recall that each scalar target quantity is (through the vector  $\mathbf{N}'$  of Eq. 2) influenced by its own one-dimensional sub-space of the parameter space, i.e. a *target direction* in parameter space. Likewise each scalar observation constrains a direction in parameter space (*observed direction*). We can use the analogy of a *perspective* under which the target direction is observed. If the target and observed directions are orthogonal, the observation can not reduce the uncertainty in the target quantity. If both directions are collinear, i.e. in the same subspace of the parameter space, the observation can most efficiently reduce the uncertainty in the target quantity. Even a hypothetically perfect measurement that removed all uncertainty for all parameters pertinent to one PFT would not completely constrain any of our target quantities (which are all influenced by several PFTs). In other words a one-site flux network is *incomplete* with respect to our target quantities. The strength of an observational constraint on a target quantity depends 1) on the sensitivity of the observed quantity to a parameter change in the observed direction (*signal size*), 2) on how well the observed direction projects onto the target direction (*perspective*), and 3) on the data uncertainty. We use the same data uncertainty for both sites and the same target directions. The observed direction and signal size depend 1) on the PFT, 2) on the sampling time, and on 3) the meteorological driving data. Our two flux sites provide measurements at the same times (hourly for 20 yr) and of the same PFT. The only different factors are the meteorological driving data. Indeed the meteorology in Southern Spain is quite different from Scandinavia.

To isolate the effects of the perspective and the signal size on performance of the individual sites we reduce their respective data uncertainties by a factor of 100 (green and brown bars in Fig. 4). This can compensate for a weaker signal but does not

## Observing the continental-scale carbon balance

T. Kaminski et al.

Title Page

Abstract

Introduction

Conclusions

References

Tables

Figures



Back

Close

Full Screen / Esc

Printer-friendly Version

Interactive Discussion



change the perspective. Now both sites show exactly the same performance, i.e. the Scandinavian site has just a smaller signal. In other words, we find the relevant information at both sites, but at sites with a larger signal we can afford a larger data uncertainty or, probably, a shorter observational period.

5 A common property between all networks evaluated in Fig. 4 is the larger uncertainty reduction for NPP compared to NEP. This happens although we sample hourly NEP, i.e. we should match the perspective for long-term NEP. On the other hand, the target space for NPP has fewer dimensions, because it depends on fewer parameters. The extra parameters in NEP play an important role. This effect would be even more pronounced if NEP was compared with the Gross Primary Productivity (GPP) which is  
10 influenced by even fewer parameters (Koffi et al., 2012). Another point to note is that for Brazil the prior uncertainty in NPP is about four times higher than for NEP, and thus easier to reduce.

## 4.2 Base networks and their combinations

15 The performance of the three base networks *flask* (blue bars), *cont* (orange bars), and *flux* (yellow bars) is shown in Fig. 6. Over Europe, the flux network achieves an uncertainty reduction of about 99% for both NEP and NPP and outperforms both atmospheric networks. The reason for the strong performance of *flux* over Europe is its completeness with respect to the European target quantities, i.e. the fact that for  
20 each PFT over Europe it contains a dedicated site. With respect to the Brazilian target quantities, in turn, the network *flux* is incomplete because it does not cover the tropical PFTs. This is why *flux* is weaker than the global network *flask*, in particular for NEP where the performance difference between both networks is over 50 percentage points.

The above suggests we would always attempt complete flux networks. In reality this  
25 may be hard to achieve, because we do not know how many PFTs are required to simulate the terrestrial carbon cycle. Hence, it may happen that we accidentally miss a PFT in our flux network. We can test the effect of this by removing from network *flux* the site “1731-9” (network *flux-C3*). The performance over Europe drops by about 69

### Observing the continental-scale carbon balance

T. Kaminski et al.

Title Page

Abstract

Introduction

Conclusions

References

Tables

Figures



Back

Close

Full Screen / Esc

Printer-friendly Version

Interactive Discussion



percentage points for NEP and 58 for NPP (green bars). Over Brazil the effect of missing the C3 grass site is only marginal (performance drop of less than four percentage points for NEP and less than two for NPP).

For the atmospheric networks, *flask* outperforms *cont* over Europe by 2 and 10 percentage points for NEP and NPP despite the European focus of *cont*. Obviously, for the atmosphere, the large-scale information matters. For Brazil or Russia it is not surprising that the global network *flask* is more powerful than the network *cont*. The most important aspect is that the atmospheric networks outperform the incomplete flux network *flux-C3*. The only exception is NPP over Brazil, where the loss of C3 had only a marginal effect on the performance of the flux network and *flux-C3* is stronger than *cont* but not than *flask*. We note that the relatively coarse resolution of TM2 may yield a slight overestimation in the integrative capacity of *flask*. For any given monthly mean sample, the higher resolution of LMDZ would resolve a finer influence structure (footprint) within the TM2 grid cells. On the other hand, our sampling period of 20 yr would probably average out much of this time-dependent fine-scale structure.

To assess the *complementarity* of atmospheric and flux networks, we combine the networks *flux-C3* and *flask*. Over Europe the resulting network *flux-C3* + *flask* performs almost as well as the *complete* flux network *flux*, and over Brazil and Russia even better. Both networks (*flux-C3* and *flask*) complement each other. Given the experience from the two grass sites we evaluated initially (Sect. 4.1), we can think of the atmospheric network as an observer of averages over multiple sites. We can regard its addition to the flux network as an insurance against the *incompleteness* of the flux network.

What can we do in the case where we can not afford enough sites to sample all PFTs over our target region? Is it useful to have a flux site which observes two PFTs? We test this by removing the site “site1731-9” from the network *flux* and modify the PFT fractions at site “site143-9” to 50 % each for PFTs 5 and 9. This network has the same number of sites as *flux-C3* but much better performance. Uncertainty reduction for NEP over Europe is 76 %, and for the other target quantities the performance is

## Observing the continental-scale carbon balance

T. Kaminski et al.

Title Page

Abstract

Introduction

Conclusions

References

Tables

Figures

◀

▶

◀

▶

Back

Close

Full Screen / Esc

Printer-friendly Version

Interactive Discussion



only marginally (less than one percentage point) inferior to *flux*. This performance enhancement is based on the same principle as atmospheric sampling, the integration of a multi-PFT signal. This result seems surprising. It arises from the ability of a long time series to observe the different dynamics of the two underlying PFTs.

5 We can also investigate the complementarity of the base networks. Since the uncertainty reduction for the network *flux* is above 99 % already, in this set of assessments we rather quantify the performance gain by the reduction in posterior uncertainty relative to the posterior uncertainty of *flux*. Adding both atmospheric networks to network *flux* reduces NEP uncertainty over Europe by over 30 % and NPP by 20 %. For the  
10 other regions the effect is much larger (up to 99 % reduction for NEP over Brazil).

### 4.3 Increased model complexity

The above network evaluations are based on a model setup with 13 PFTs. In the following we investigate the robustness of the results with respect to model complexity in terms of the number of available PFTs. We can do this in an efficient manner by splitting the vegetation into several copies. Each copy has its own set of 57 independent  
15 parameters with uncorrelated prior uncertainty. All copies of a PFT share the location of the original PFT. In the following we will call the number of copies *multiplicity*. With multiplicity 4, for example, we have  $4 \times 13 = 52$  PFTs and  $57 \times 4 = 228$  parameters. In this case there are no global parameters. A change of multiplicity also affects the prior  
20 uncertainty in the target quantities. Introducing the multiplicity  $m$  means that  $m$  copies have to share the same area. Hence, compared to the original flux  $y$  the flux  $y_i$  from each copy ( $i$  counting the copies) is reduced by a factor of  $m$ . And with it the original flux uncertainty  $\sigma(y_{\text{prior}})$  is also reduced by a factor of  $m$  for each copy  $\sigma(y_{i,\text{prior}})$ . Since there is no correlation of the prior uncertainty among the copies, the total flux

## Observing the continental-scale carbon balance

T. Kaminski et al.

Title Page

Abstract

Introduction

Conclusions

References

Tables

Figures



Back

Close

Full Screen / Esc

Printer-friendly Version

Interactive Discussion



uncertainty  $\sigma(y_{\text{prior},m})$  is the square root of the sum of squares:

$$\sigma(y_{\text{prior},m}) = \sqrt{\sum_{i=1,m} \sigma(y_{i,\text{prior}})^2} = \sqrt{\sum_{i=1,m} \left(\frac{\sigma(y_{\text{prior}})}{m}\right)^2} = \frac{\sigma(y_{\text{prior}})}{\sqrt{m}}. \quad (5)$$

This means, for example, quadrupling the multiplicity halves the prior uncertainty.

For multiplicity 4, Fig. 7 shows the performance of the three base networks. Among the atmospheric networks *flask* is superior to *cont* for all target quantities, except for NEP over Europe where *flask* is slightly inferior. The network *flux*, in turn, is superior to *flask* except for NEP over Brazil and Russia. We define the network *M4-1 flux*, which is incomplete over Europe, by excluding one parameter copy out of the 4 from the network *flux*. This means *M4-1 flux* samples 30 out of the 40 PFTs that are available over Europe. As in the case of multiplicity 1, the incompleteness is reflected in a strong drop in uncertainty reduction in particular over Europe, where the performance is roughly halved (green bars in Fig. 7). Combining *M4-1 flux* with *flask* is only marginally superior to *flask* alone. Apparently *M4-1 flux* is too incomplete to bring extra information. Put another way, the unobserved parts of the domain dominate the final uncertainty.

For multiplicity 25, *flux* achieves uncertainty reductions close to 100 % over Europe and above 85 % elsewhere. We define two incomplete flux networks over Europe, one with one parameter copy out of 25 removed (over Europe 240 of 250 PFTs sampled) and the other one with two parameter copies out of 25 removed (230 PFTs sampled). Over Europe, compared to *flux*, the first network suffers a performance drop of about 20 percentage points, and the other one of almost 30 percentage points. Over Europe the *flask* performance lies in-between both incomplete flux networks, which also holds for NPP over Russia. Elsewhere *flask* is better than the two networks. Even with a highly increased number of PFTs, an incomplete flux network that misses only a small fraction of the total PFTs is outperformed by *flask*. Combining *flask* with either one of the incomplete networks increases the *flask* performance over Europe by about ten percentage points for the smaller flux network and by another three percentage

## Observing the continental-scale carbon balance

T. Kaminski et al.

Title Page

Abstract

Introduction

Conclusions

References

Tables

Figures



Back

Close

Full Screen / Esc

Printer-friendly Version

Interactive Discussion



points for the larger network. This means both incomplete networks exhibit enough complementarity to *flask* to achieve a significant performance gain.

## 5 Conclusions

QND is well-suited to explore the performance of observational networks of the carbon cycle. The network designer is a fast and easy-to-use QND implementation, that enables interactive network evaluations, e.g. within a meeting. Figures 2, 3 and 5 in this paper are directly obtained from the network designer.

As mentioned above the particular performance values are consequences of specific choices such as the complexity of the underlying terrestrial model. There are, however, a set of general findings that follow from the above-mentioned assumption of fundamental equations that govern the processes controlling the terrestrial carbon fluxes. First, for direct flux observations, it is important to cover the full range of different PFTs and not the range of climates to which a given PFT is exposed. An incomplete flux network, i.e. one that misses a fraction of the PFTs risks a considerable performance loss. Atmospheric measurements are less prone to this problem, thus we can say that flux networks are more powerful while concentration networks are more robust. The combination can provide both qualities, i.e. atmospheric and flux networks complement each other.

The implications for the design of integrated observing strategies for the continental carbon balance seem clear. The baseline requirement is an atmospheric sampling network. That way if we underestimate the heterogeneity we will not find ourselves suddenly terribly undersampled. The strongest constraint, however, will come by overlaying this with a flux network which is as comprehensive as possible. Oversampling important PFTs will also give a diagnostic of heterogeneity. If parameters retrieved from one flux site enable us to predict the fluxes at a second then these are properly considered the same PFT for CCDAS, otherwise we need to increase the multiplicity.

## Observing the continental-scale carbon balance

T. Kaminski et al.

Title Page

Abstract

Introduction

Conclusions

References

Tables

Figures

◀

▶

◀

▶

Back

Close

Full Screen / Esc

Printer-friendly Version

Interactive Discussion



**Observing the  
continental-scale  
carbon balance**

T. Kaminski et al.

Title Page

Abstract

Introduction

Conclusions

References

Tables

Figures

◀

▶

◀

▶

Back

Close

Full Screen / Esc

Printer-friendly Version

Interactive Discussion



This study addressed parametric and, to a certain extent, initial value uncertainty. To resolve structural uncertainty, it is important to build into the network the flexibility to detect features that are not or badly included in the model, i.e. the capability to discover surprises. Here, we have focused on carbon dioxide fluxes, however, observational networks for other trace gases, e.g. methane, can be evaluated with the same approach. Also, it is possible to evaluate networks that combine observations from space with in situ measurements as shown by Kaminski et al. (2010) and Kaminski et al. (2011). The approach can also be extended to oceanic networks.

*Acknowledgements.* This work was supported in part by the European Community within the 6th Framework Programme for Research and Technological Development under contract no. 026188. PR is in receipt of an ARC Professorial Fellowship (DP1096309).

**References**

- Carouge, C., Bousquet, P., Peylin, P., Rayner, P. J., and Ciais, P.: What can we learn from European continuous atmospheric CO<sub>2</sub> measurements to quantify regional fluxes – Part 1: Potential of the 2001 network, *Atmos. Chem. Phys.*, 10, 3107–3117, doi:10.5194/acp-10-3107-2010, 2010a. 7216
- Carouge, C., Rayner, P. J., Peylin, P., Bousquet, P., Chevallier, F., and Ciais, P.: What can we learn from European continuous atmospheric CO<sub>2</sub> measurements to quantify regional fluxes – Part 2: Sensitivity of flux accuracy to inverse setup, *Atmos. Chem. Phys.*, 10, 3119–3129, doi:10.5194/acp-10-3119-2010, 2010b. 7216
- Enting, I. G.: *Inverse Problems in Atmospheric Constituent Transport*, Cambridge University Press, Cambridge, 2002. 7212
- Giering, R. and Kaminski, T.: Recipes for adjoint code construction, *ACM T. Math. Software*, 24, 437–474, 1998. 7217
- Gurney, K. R., Law, R. M., Denning, A. S., Rayner, P. J., Baker, D., Bousquet, P., Bruhwiler, L., Chen, Y.-H., Ciais, P., Fan, S., Fung, I. Y., Gloor, M., Heimann, M., Higuchi, K., John, J., Maki, T., Maksyutov, S., Masarie, K., Peylin, P., Prather, M., Pak, B. C., Randerson, J., Sarmiento, J., Taguchi, S., Takahashi, T., and Yuen, C.-W.: Towards robust regional esti-

**Observing the  
continental-scale  
carbon balance**

T. Kaminski et al.

Title Page

Abstract

Introduction

Conclusions

References

Tables

Figures

◀

▶

◀

▶

Back

Close

Full Screen / Esc

Printer-friendly Version

Interactive Discussion



mates of CO<sub>2</sub> sources and sinks using atmospheric transport models, *Nature*, 415, 626–630, 2002. 7212

Hardt, M. and Scherbaum, F.: The design of optimum networks for aftershock recordings, *Geophys. J. Int.*, 117, 716–726, 1994. 7213

5 Hauglustaine, D. A., Hourdin, F., Jourdain, L., Filiberti, M. A., Walters, S., Lamarque, J. F., and Holland, E. A.: Interactive chemistry in the Laboratoire de Météorologie Dynamique general circulation model: description and background tropospheric chemistry evaluation, *J. Geophys. Res.*, 109, 44 pp., doi:10.1029/2003JD003957, 2004. 7216

Heimann, M.: The Global Atmospheric Tracer Model TM2, Technical Report No. 10, Max-Planck-Institut für Meteorologie, Hamburg, Germany, 1995. 7216

Kaminski, T. and Rayner, P. J.: Assimilation and network design, in: *Observing the Continental Scale Greenhouse Gas Balance of Europe*, edited by: Dolman, H., Freibauer, A., and Valentini, R., *Ecological Studies*, chap. 3, Springer-Verlag, New York, 2008. 7214, 7218

15 Kaminski, T., Heimann, M., and Giering, R.: A coarse grid three dimensional global inverse model of the atmospheric transport, 1, Adjoint Model and Jacobian Matrix, *J. Geophys. Res.*, 104, 18535–18553, 1999. 7220

Kaminski, T., Knorr, W., Rayner, P. J., and Heimann, M.: Assimilating atmospheric data into a terrestrial biosphere model: a case study of the seasonal cycle, *Global Biogeochem. Cy.*, 16, 14-1–14-16, available online at: <http://www.agu.org/journals/gb/gb0204/2001GB001463/index.html>, 2002. 7213, 7220

20 Kaminski, T., Scholze, M., and Houweling, S.: Quantifying the benefit of A-SCOPE data for reducing uncertainties in terrestrial carbon fluxes in CCDAS, *Tellus B*, 62, 784–796, doi:10.1111/j.1600-0889.2010.00483.x, available at: <http://journals.sfu.ca/coaction/index.php/tellusb/article/view/16634>, 2010. 7214, 7218, 7228

25 Kaminski, T., Knorr, W., Scholze, M., Gobron, N., Pinty, B., Giering, R., and Mathieu, P.-P.: Consistent assimilation of MERIS FAPAR and atmospheric CO<sub>2</sub> into a terrestrial vegetation model and interactive mission benefit analysis, *Biogeosciences Discuss.*, 8, 10761–10795, doi:10.5194/bgd-8-10761-2011, 2011. 7214, 7228

Knorr, W.: Annual and interannual CO<sub>2</sub> exchanges of the terrestrial biosphere: process-based simulations and uncertainties, *Global Ecol. Biogeogr.*, 9, 225–252, 2000. 7215

30 Knorr, W. and Heimann, M.: Uncertainties in global terrestrial biosphere modeling: 1. A comprehensive sensitivity analysis with a new photosynthesis and energy balance scheme, *Global Biogeochem. Cy.*, 15, 207–225, 2001. 7215

- Knorr, W. and Kattge, J.: Inversion of terrestrial biosphere model parameter values against eddy covariance measurements using Monte Carlo sampling, *Glob. Change Biol.*, 11, 1333–1351, 2005. 7219
- Koffi, E., Rayner, P. J., Scholze, M., and Beer, C.: Atmospheric constraints on gross primary productivity and net flux: results from a carbon-cycle data assimilation system, *Global Biogeochem. Cy.*, 26, doi:10.1029/2010GB003900, in press, 2012. 7214, 7223
- Nijssen, B., Schnur, R., and Lettenmaier, D.: Retrospective estimation of soil moisture using the VIC land surface model, 1980–1993, *J. Climate*, 14, 1790–1808, 2001. 7215
- Rayner, P. J., Scholze, M., Knorr, W., Kaminski, T., Giering, R., and Widmann, H.: Two decades of terrestrial Carbon fluxes from a Carbon Cycle Data Assimilation System (CCDAS), *Global Biogeochem. Cy.*, 19, 20 pp., doi:10.1029/2004GB002254, available online at: <http://www.agu.org/pubs/crossref/2005/2004GB002254.shtml>, 2005. 7214, 7215, 7216, 7232, 7236
- Rayner, P. J., Koffi, E., Scholze, M., Kaminski, T., and Dufresne, J.: Constraining predictions of the carbon cycle using data, *Philos. T. R. Soc. A*, 369, 1955–1966, doi:10.1098/rsta.2010.0378, available online at: <http://rsta.royalsocietypublishing.org/content/369/1943/1955.abstract>, 2011. 7214
- Rayner, P. J.: The current state of carbon-cycle data assimilation, *Current Opinion in Environmental Sustainability*, 2, 289–296, doi:10.1016/j.cosust.2010.05.005, available online at: <http://www.sciencedirect.com/science/article/pii/S1877343510000370>, 2010. 7213
- Rayner, P. J. and O'Brien, D. M.: The utility of remotely sensed CO<sub>2</sub> concentration data in surface source inversions, *Geophys. Res. Lett.*, 28, 175–178, 2001. 7214
- Rayner, P. J., Enting, I. G., and Trudinger, C. M.: Optimizing the CO<sub>2</sub> observing network for constraining sources and sinks, *Tellus B*, 48, 433–444, 1996. 7214
- Rayner, P. J., Enting, I. G., Francey, R. J., and Langenfelds, R. L.: Reconstructing the recent carbon cycle from atmospheric CO<sub>2</sub>,  $\delta^{13}\text{C}$  and O<sub>2</sub>/N<sub>2</sub> observations, *Tellus B*, 51, 213–232, 1999. 7212
- Scholze, M., Kaminski, T., Rayner, P. J., Knorr, W., and Giering, R.: Propagating uncertainty through prognostic CCDAS simulations, *J. Geophys. Res.*, 112, 13 pp., doi:10.1029/2007JD008642, 2007. 7214, 7215, 7216, 7218
- Solomon, S., Qin, D., Manning, M., Chen, Z., Marquis, M., Averyt, K., Tignor, M., and Miller, H.: IPCC, 2007: Climate Change 2007: The Physical Science Basis, Contribution of Working Group I to the Fourth Assessment Report of the Intergovernmental Panel on Climate Change, Cambridge University Press, Cambridge, United Kingdom and New York, NY, USA,

**Observing the  
continental-scale  
carbon balance**

T. Kaminski et al.

Title Page

Abstract

Introduction

Conclusions

References

Tables

Figures

◀

▶

◀

▶

Back

Close

Full Screen / Esc

Printer-friendly Version

Interactive Discussion



2007. 7212

Wilson, M. F. and Henderson-Sellers, A.: A global archive of land cover and soils data for use in general-circulation climate models, J. Climatol., 5, 119–143, 1985. 7215

Discussion Paper | Discussion Paper | Discussion Paper | Discussion Paper | Discussion Paper

ACPD

12, 7211–7242, 2012

---

**Observing the  
continental-scale  
carbon balance**

T. Kaminski et al.

---

Title Page

Abstract

Introduction

Conclusions

References

Tables

Figures



Back

Close

Full Screen / Esc

Printer-friendly Version

Interactive Discussion



## Observing the continental-scale carbon balance

T. Kaminski et al.

**Table 1.** Plant Functional Types (PFTs) defined in CCDAS and their abbreviations, taken from Rayner et al. (2005).

PFT No.	PFT Name	Abbreviation
0	Not vegetated	
1	Trop. broadleaved evergreen tree	TrEv
2	Trop. broadleaved deciduous tree	TrDec
3	Temp. broadleaved evergreen tree	TmpEv
4	Temp. broadleaved deciduous tree	TmpDec
5	Evergreen coniferous tree	EvCn
6	Deciduous coniferous tree	DecCn
7	Evergreen shrub	EvShr
8	Deciduous shrub	DecShr
9	C3 grass	C3Gr
10	C4 grass	C4Gr
11	Tundra vegetation	Tund
12	Swamp vegetation	Wetl
13	Crops	Crop

Title Page

Abstract

Introduction

Conclusions

References

Tables

Figures

◀

▶

◀

▶

Back

Close

Full Screen / Esc

Printer-friendly Version

Interactive Discussion





## Observing the continental-scale carbon balance

T. Kaminski et al.

Title Page

Abstract

Introduction

Conclusions

References

Tables

Figures

◀

▶

◀

▶

Back

Close

Full Screen / Esc

Printer-friendly Version

Interactive Discussion



**Table 3.** Network *flux*. First number in site name indicates model grid cell and second number PFT.

Name	Included	Uncertainty [ $\text{gC m}^{-2} \text{day}^{-1}$ ]	lon	lat
site1413-3	yes	10.0	9.0	45.0
site1025-4	yes	10.0	35.0	53.0
site143-5	yes	10.0	19.0	69.0
site148-7	yes	10.0	29.0	69.0
site1495-8	yes	10.0	-5.0	43.0
site1731-9	yes	10.0	-5.0	37.0
site1578-10	yes	10.0	-5.0	41.0
site377-11	yes	10.0	-21.0	65.0
site388-12	yes	10.0	29.0	65.0
site621-13	yes	10.0	13.0	61.0

## Observing the continental-scale carbon balance

T. Kaminski et al.

Title Page

Abstract

Introduction

Conclusions

References

Tables

Figures

◀

▶

◀

▶

Back

Close

Full Screen / Esc

Printer-friendly Version

Interactive Discussion



**Table 4.** Network *cont* of continuous atmospheric sampling sites over Europe.

Name	Included	Uncertainty	lon	lat
CBW	yes	1.5	4.9	52.0
CMN	yes	1.5	10.7	44.1
DGR	yes	1.5	22.07	54.15
FDA	yes	1.5	25.3	45.47
HUN	yes	1.5	16.6	46.9
MHD	yes	1.5	−9.9	53.33
NGB	yes	1.5	13.05	53.15
PAL	yes	1.5	24.12	67.97
PRS	yes	1.5	7.7	45.9
PUY	yes	1.5	3.0	45.8
SAC	yes	1.5	2.2	48.7
SBK	yes	1.5	12.98	47.05
SCH	yes	1.5	8.0	48.0
WES	yes	1.5	8.0	55.0
WHF	yes	1.5	10.77	52.8

**Observing the  
continental-scale  
carbon balance**

T. Kaminski et al.

Title Page

Abstract

Introduction

Conclusions

References

Tables

Figures

◀

▶

◀

▶

Back

Close

Full Screen / Esc

Printer-friendly Version

Interactive Discussion

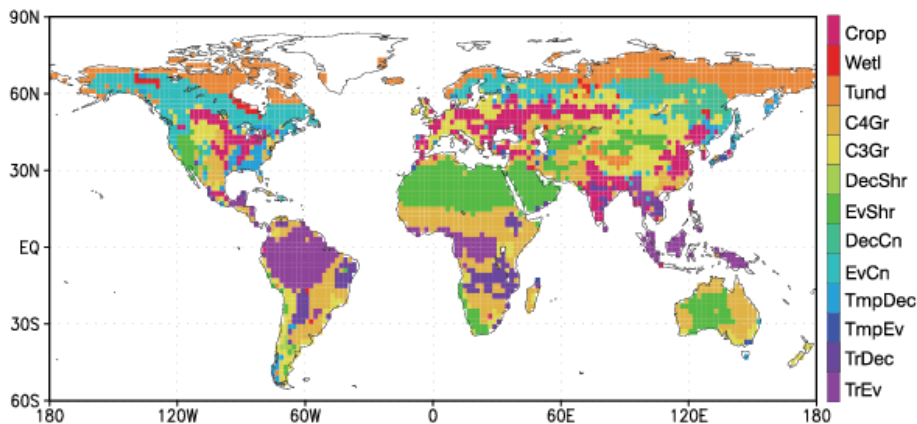
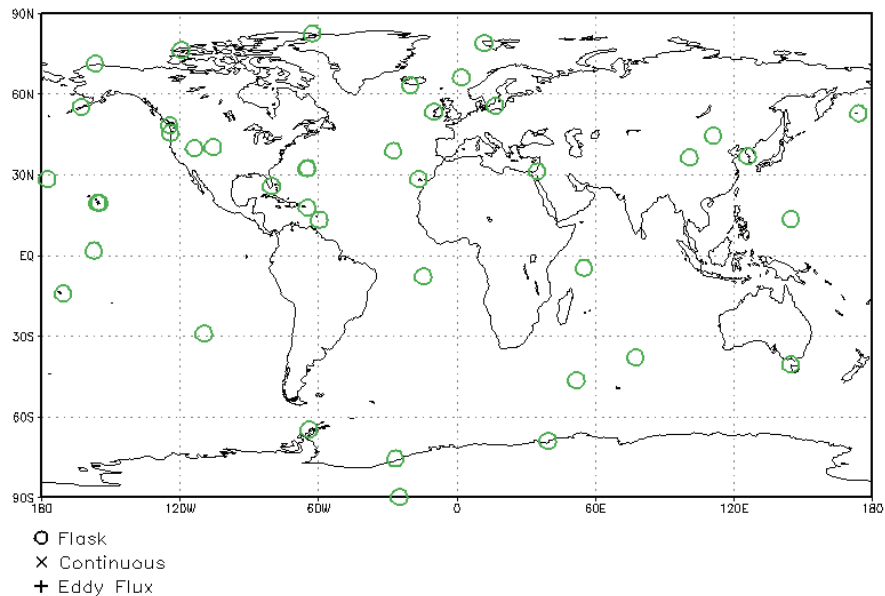


**Fig. 1.** Distribution of the dominant CCDAS Plant Functional Type (PFT) per grid cell, PFT labels are given in Table 1, taken from Rayner et al. (2005).



GRADS: COLA/IGES

2011-09-20-17:12

**Fig. 2.** Observational network *flask* providing atmospheric flask samples.

**Observing the continental-scale carbon balance**

T. Kaminski et al.

Title Page

Abstract

Introduction

Conclusions

References

Tables

Figures

◀

▶

◀

▶

Back

Close

Full Screen / Esc

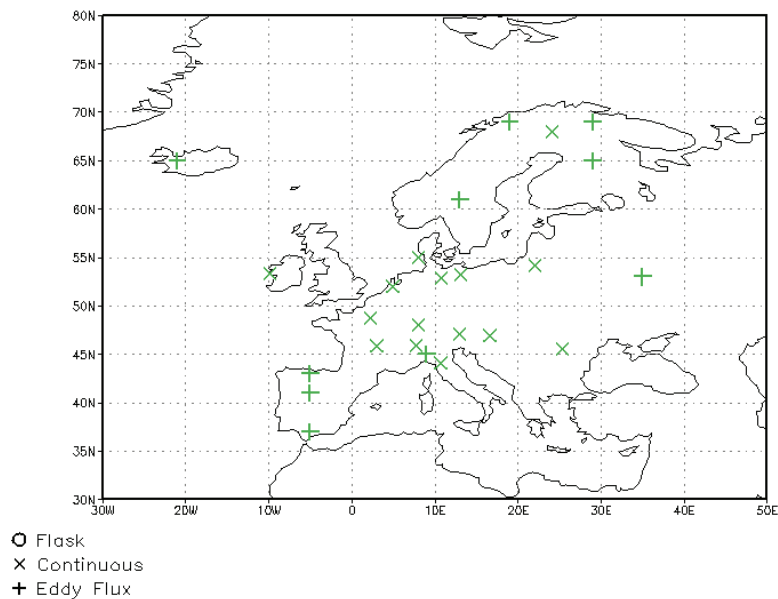
Printer-friendly Version

Interactive Discussion



## Observing the continental-scale carbon balance

T. Kaminski et al.



gRADS: COLA/IGES

2012-01-30-16:57

**Fig. 3.** Observational networks *flux* (+) providing flux measurements and *cont* (X) providing atmospheric flask samples.

Title Page

Abstract

Introduction

Conclusions

References

Tables

Figures

◀

▶

◀

▶

Back

Close

Full Screen / Esc

Printer-friendly Version

Interactive Discussion



## Observing the continental-scale carbon balance

T. Kaminski et al.

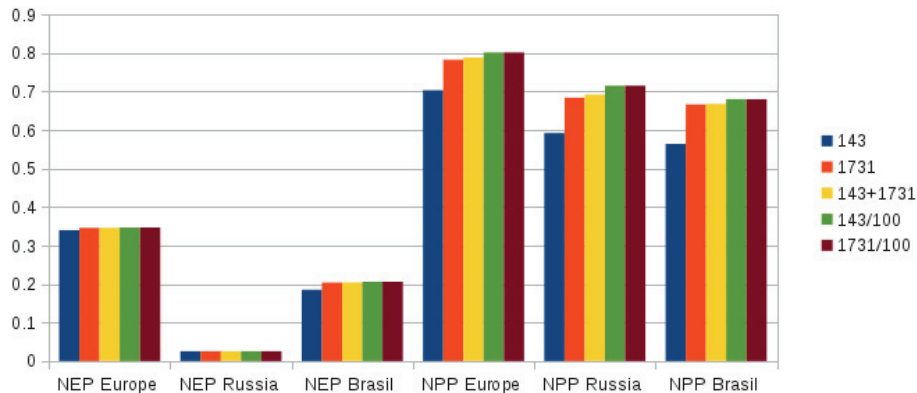


**Fig. 4.** Evaluation of two flux sites (blue and orange bars), of their combination (yellow bars), and of each site with data uncertainty reduced by a factor of 100 (green and brown bars): Uncertainty reduction for NEP and NPP integrated over three regions.

Title Page

Abstract

Introduction

Conclusions

References

Tables

Figures

◀

▶

◀

▶

Back

Close

Full Screen / Esc

Printer-friendly Version

Interactive Discussion



**Observing the  
continental-scale  
carbon balance**

T. Kaminski et al.

Title Page

Abstract

Introduction

Conclusions

References

Tables

Figures



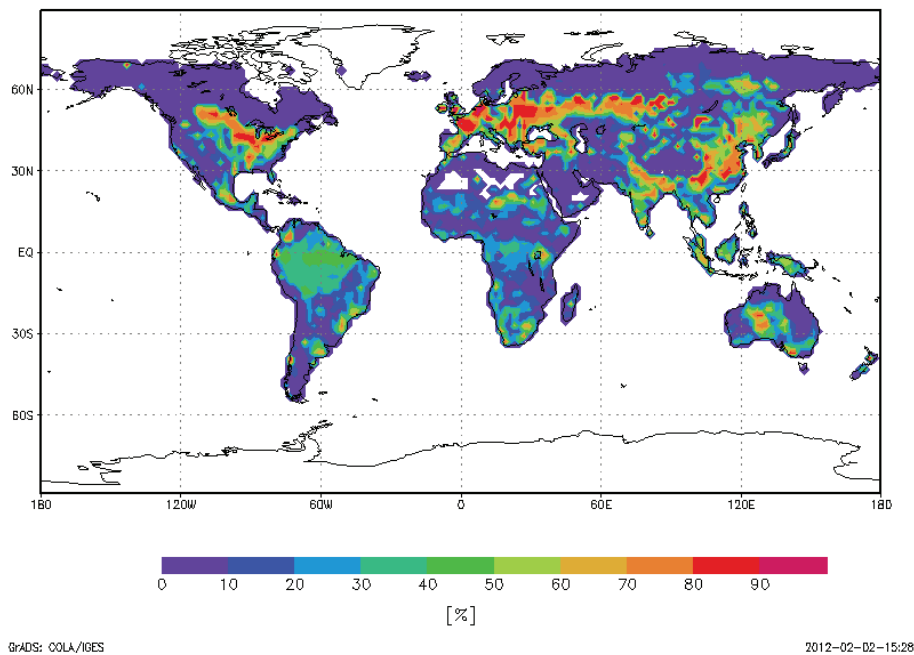
Back

Close

Full Screen / Esc

Printer-friendly Version

Interactive Discussion

**Fig. 5.** Uncertainty reduction in NEP per grid cell.

## Observing the continental-scale carbon balance

T. Kaminski et al.

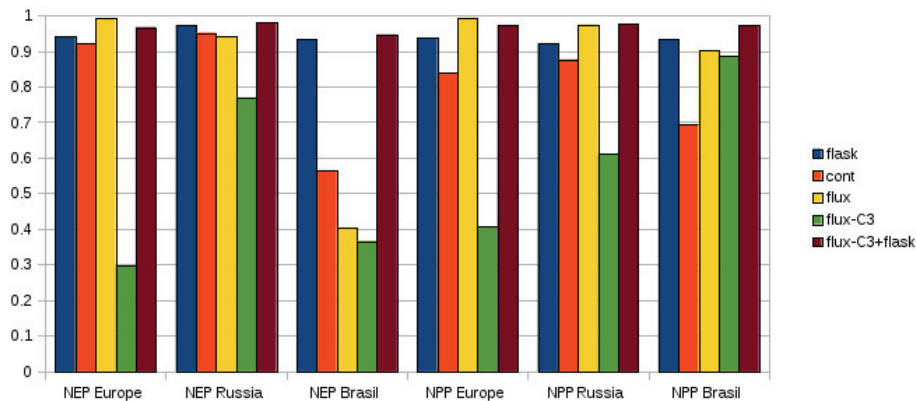


**Fig. 6.** Evaluation of three base networks, a flux network *flux-C3* that is incomplete over Europe and the combined *flux-C3 + flask* network.

Title Page

Abstract

Introduction

Conclusions

References

Tables

Figures

⏪

⏩

◀

▶

Back

Close

Full Screen / Esc

Printer-friendly Version

Interactive Discussion



## Observing the continental-scale carbon balance

T. Kaminski et al.

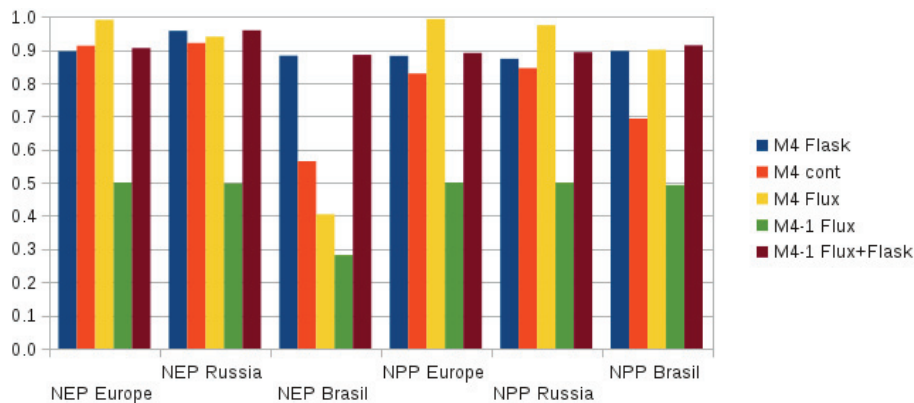


**Fig. 7.** Evaluation for multiplicity 4 of three base networks and an incomplete flux network with one copy of each PFT unsampled.

Title Page

Abstract

Introduction

Conclusions

References

Tables

Figures

◀

▶

◀

▶

Back

Close

Full Screen / Esc

Printer-friendly Version

Interactive Discussion

